12AFMC, Sydney 1995 pp. 473-476

THE EFFECT OF ASPECT RATIO AND DIVERGENCE ON THE TURBULENCE STRUCTURE OF BOUNDARY LAYERS

M. B. Jones, Ivan Marusic and A. E. Perry
Department of Mechanical and Manufacturing Engineering
University of Melbourne
Parkville, Victoria
AUSTRALIA

ABSTRACT

The effect of the aspect ratio of a turbulent boundary layer on the mean flow, broadband turbulence intensities and Reynolds shear stress has been studied. The aspect ratio (AR) is defined as the boundary layer thickness divided by the boundary layer width, i.e. the effective wind tunnel width. Measurements have been taken in a nominally zero pressure gradient layer at a single station for three different aspect ratio settings, $AR = 1/4$, $AR = 1/7$, and $AR = 1/13$. The measurements show that the turbulent quantities were unaffected when the aspect ratio was increased from $AR = 1/13$ to $AR = 1/7$. However at $AR = 1/4$ there appears to be a slight increase in the broadband turbulence intensities and Reynolds shear stress.

INTRODUCTION

There has been little attention paid to the effect aspect ratio may have on the structure of the flow. For example Stratford (1959) encountered high aspect ratio boundary layers in his experiments, such as $AR = 1/2$. Stratford claims to have ensured that two dimensionality in the mean was maintained, but the question of whether the flow structure was affected remains unanswered. Another example is a high Reynolds number wind tunnel designed (but not yet built) at the University of Melbourne. This tunnel has the potential to produce high AR layers. It is desirable to know how far downstream one can measure (eg. how large the AR can grow to) before aspect ratio effects may be a problem.

EXPERIMENTAL SET-UP

Experiments were performed in an open return blower wind tunnel, with a working section of 4.4 m length. The contraction area ratio before the working section is 8.9 : 1, with an initial working section area 940 mm wide by 388 mm high. The freestream turbulence level was less than 0.5%. The boundary layer studied develops on the smooth acrylic floor of the working section and is tripped using a 0.8 mm diameter trip wire.

In order to change the aspect ratio whilst maintaining constant Reynolds number, false walls were fitted inside the working section and ran the entire length of the working section. The position of these walls were adjusted to achieve the $AR = 1/4$ and $AR = 1/7$ cases while for the $AR = 1/13$ case these walls were removed altogether. Care was taken to ensure that the flow did not separate at the leading edge of these false walls, by fitting nose aerofoils to them. A triangular cornice was placed along the bottom edge of the walls to discourage secondary flows.

The C_p distribution was controlled by hinging the rigid ceiling to allow for boundary layer growth whilst maintaining nominally zero pressure gradient streamwise conditions. Here C_p is defined as

$$C_p = 1 - (U_1/U_\infty)^2$$

where U_1 is the freestream velocity and U_∞ is the reference freestream velocity. The distribution was measured by use of pressure tappings along the centre-line length of the working section. For the case where the tunnel was run with the walls removed ($AR = 1/13$) the variation of C_p was within $\pm 0.5\%$. However when the false walls were inserted, the C_p could be kept only within $\pm 1.5\%$. It is felt that this is due to some waviness present in these false walls.

The tunnel was run at a nominal freestream velocity of 20 m/s but this varied from day to day to keep the measuring station Reynolds number constant at $Re = U_1 x/\nu = 4.882 \times 10^9 \pm 1.0\%$. Here x is the

distance downstream of the trip wire and ν is the fluid kinematic viscosity.

Two dimensionality in the mean was checked by taking spanwise traverses and measuring the V (spanwise) component. For the $AR = 1/7$ case a traverse was taken at a level $z = 0.5 \times \delta_c$ and $z = 2 \times \delta_c$. Inside the layer the maximum variation in V/U was ± 0.006 and outside it was ± 0.005 over a span of 400 mm about the centre-line.

Mean profiles were measured using a Pitot-static probe, in conjunction with a MKS Baratron 170M-6C manometer. The Pitot-static probe was calibrated against an N.P.L standard.

Broadband turbulence intensities and Reynolds shear stresses were measured using constant temperature hot-wire anemometers. A cross wire probe was used with wires inclined nominally at angles of $\pm 45^o$ to the streamwise direction and etched to a length of 1.0 mm. The square-wave response of the anemometer was adjusted for optimum damping giving a frequency response of 20kHz or greater, over the range of velocities encountered. Wires were calibrated dynamically by using the method given in Perry (1982). The calibration was checked by shaking the probe at a known frequency in the horizontal and vertical directions the errors in $\overline{u_1^2}$ and $\overline{u_3^2}$ were within 2.0% and the errors in mean velocity were within 0.8%. Here u_1, u_2 and u_3 are the fluctuating velocity components in the streamwise (x), spanwise (y) and wall-normal (z) directions respectively and overbars denote temporal averages. The wires were calibrated before each traverse and the temperature variation between the calibration and the end of the run was kept to within 1.5°C.

RESULTS

Mean Flow

The mean flow profiles for the three cases are plotted in figure 1. Here U is the mean velocity in the streamwise direction and U_τ is the wall shear velocity calculated using the Clauser chart method. All cases collapse onto the law of the wall as shown in the turbulent wall region. Using Coles (1956) law of the wall; law of the wake formulation given by equation (1) the important mean flow parameters can be calculated and are given in table 1. Here $\eta = z/\delta_c$, δ_c is the boundary layer thickness, κ is the Karman constant (assumed to be 0.41), A is the universal smooth wall constant (assumed to be 5.0), Π is the Coles wake factor and W_c is the modified Coles wake function proposed by Perry & Li (1990).

$$\frac{U}{U_\tau} = \frac{1}{\kappa} \ln \left[\frac{zU_\tau}{\nu} \right] + A + \frac{\Pi}{\kappa} W_c[\eta, \Pi] \qquad (1)$$

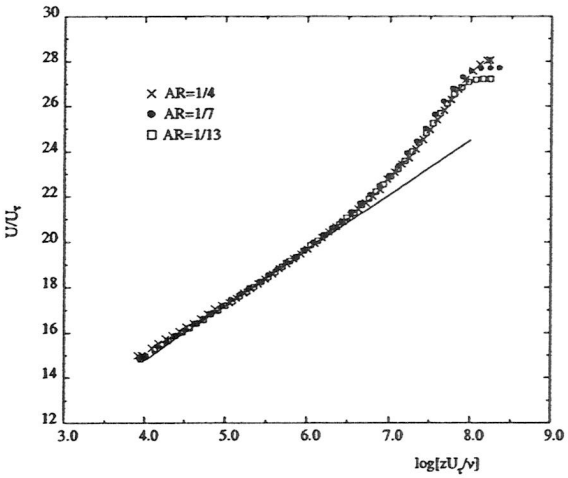

Figure 1: Mean flow profiles for different aspect ratios.

AR	δ^*/δ_c	θ/δ_c	U_τ	Π	S	R_θ	δ_c
1/4	0.129	0.09	0.738	0.629	28.11	10412	81.28
1/7	0.129	0.09	0.765	0.610	27.72	9049	70.49
1/13	0.125	0.09	0.737	0.541	27.22	8475	68.23

Table 1: Mean flow parameters for different aspect ratio conditions. Here δ^* is displacement thickness, θ is momentum thickness, $R_\theta = U_1\theta/\nu$ and $S = U_1/U_\tau$. U_τ is given in m/s while δ_c is given in mm.

Reynolds Stresses

Reynolds shear stresses are shown in figure 2 plotted both semi-logarithmically and linearly against the non-dimensional normal coordinate, z/δ_c. For the aspect ratios of 1/13 and 1/7 there are no detectable difference in the shear stress profiles. However when the aspect ratio is increased to 1/4 the shear stress profile increases by approximately 10% for $z/\delta_c > 0.05$.

Broadband turbulence intensities $\overline{u_1^2}$, $\overline{u_2^2}$ and $\overline{u_3^2}$ are shown in figures 3(a-c) respectively, they have been non-dimensionalized with the wall shear velocity U_τ and are plotted semi-logarithmically. The results for $\overline{u_1^2}/U_\tau^2$ appear unaffected between the $AR = 1/13$ and $AR = 1/7$ case while for the $AR = 1/4$ case $\overline{u_1^2}/U_\tau^2$ is approximately 5.0% higher. Figure 3(b) shows an apparent trend for $\overline{u_2^2}/U_\tau^2$ to increase with aspect ratio, although close to the wall (eg. $\eta < 0.1$) the data collapses. From Figure 3(c) it can be seen that when the AR is increased from 1/13 to 1/7 there is a slight increase in $\overline{u_3^2}/U_\tau^2$ away from the wall (eg. $\eta > 0.1$) however close to the wall (eg. $\eta < 0.1$) there is a slight decrease, although it is within experimental error. This change in profile becomes more pronounced as the AR is further increased to $AR = 1/4$.

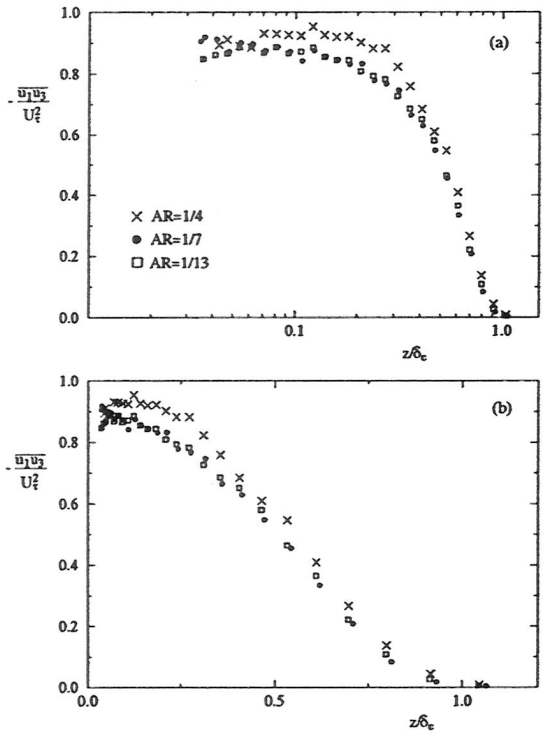

Figure 2: Reynolds shear stress profiles for different aspect ratios.

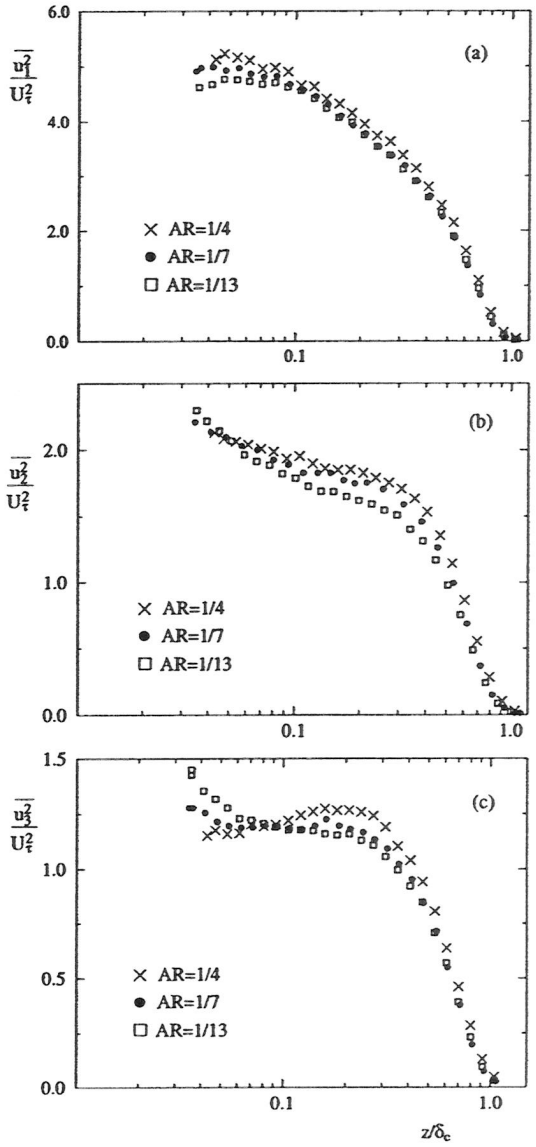

Figure 3: Broadband turbulence intensity profiles for different aspect ratios

EFFECT OF DIVERGENCE ON SHEAR STRESS

It may be possible to explain the above trends with increasing aspect ratio by considering the growth and interaction of the side-wall boundary layers developing with streamwise distance. As these side wall boundary layers encroach towards the centreline, an effective convergence strain rate will be experienced. This effect can be investigated by considering the parameter D which characterizes divergent/convergent flows. Using the definition for divergence as given by Head & Prahlad (1974) and Saddoughi (1988), that is, the divergence at a point P at a distance x on the x-axis is equal to the curvature of the equipotential line passing though that point, ie.

$$D = \frac{1}{R} = \frac{1}{x - x_0} \tag{2}$$

where x_0 is the location of the virtual sink or source.

Therefore negative values of D imply convergence and as aspect ratio is increased this will lead to an increase in the magnitude of D. It can be shown (see Saddoughi 1988) that when the plane of symmetry is considered

$$D = \frac{1}{U}\frac{\partial V}{\partial y}. \tag{3}$$

It is desirable to know if a change in D for each aspect ratio may explain the change in Reynolds shear stress.

Perry, Marusic & Li (1994) have generated an expression for the shear stress profile for two dimensional flow in the mean (ie. D=0) by using the defect law

$$\frac{U_1 - U}{U_\tau} = -\frac{1}{\kappa}\log\eta + \frac{\Pi}{\kappa}W_c[1,\Pi] - \frac{\Pi}{\kappa}W_c[\eta,\Pi] \tag{4}$$

the continuity equation

$$\frac{\partial U}{\partial x} + \frac{\partial W}{\partial z} = 0 \tag{5}$$

and the mean momentum equation for two dimensional flow in the mean

$$U\frac{\partial U}{\partial x} + W\frac{\partial U}{\partial z} = -\frac{1}{\rho}\frac{dp_1}{dx} + \frac{1}{\rho}\frac{\partial \tau}{\partial z} \tag{6}$$

where

$$\frac{\tau}{\rho} = -\overline{u'w'} + \frac{\partial U}{\partial z} \tag{7}$$

and where τ is the local shear stress. Substituting (4) and (5) into (6) and integrating gives the shear stress

profile of the form

$$\frac{\tau}{\tau_0} = f_1[\eta, \Pi, S] + f_2[\eta, \Pi, S]\delta_c \frac{d\Pi}{dx} + f_3[\eta, \Pi, S]\frac{\delta_c}{U_1}\frac{dU_1}{dx}. \quad (8)$$

Here τ_0 is the wall shear stress and $s = U_1/U_\tau$. If the above expression is extended to case where $D \neq 0$, then the continuity equation for three dimensional flow must be used instead and it is given by

$$\frac{\partial U}{\partial x} + \frac{\partial V}{\partial y} + \frac{\partial W}{\partial z} = 0. \quad (9)$$

If we are confined to the plane of symmetry it can be shown that the mean momentum equation for two dimensional flow remains a good approximation provided the spanwise gradient given by $\partial \overline{u_1 u_2}/\partial y$ is at least an order of magnitude smaller than $\partial \overline{u_1 u_3}/\partial z$. The defect law is also still applicable. So repeating the method outlined above produces a shear stress profile of the form

$$\frac{\tau}{\tau_0} = f_1[\eta, \Pi, S] + f_2[\eta, \Pi, S]\delta_c \frac{d\Pi}{dx} + f_3[\eta, \Pi, S]\frac{\delta_c}{U_1}\frac{dU_1}{dx} + f_4[\eta, \Pi, S]\delta_c D. \quad (10)$$

Figure 4 shows this shear stress profile calculated using the mean flow parameters in table 1 for different levels of convergence. Here $d\Pi/dx$ is assumed to be zero in (10). It has also been found that the shear stress profile is not sensitive to the variations in the Π values seen in table 1.

DISCUSSION AND CONCLUSIONS

The curves in figure 4 clearly show the effect that significant values of $D\delta_c$ have on the total shear stress. In order to see whether these effects could account for the trends in the experimental results, initial estimates of $D\delta_c$ were obtained by considering the effect of displacement thickness growth of the side wall boundary layers. However, these estimates proved to be very small and could not explain the trends. The value of $D\delta_c$ as deduced from spanwise V/U measurements was -0.003 for $AR = 1/7$. The value of $D\delta_c$ as calculated by considering the effects of displacement thickness was -0.0005. It can be seen from figures 4(a) and (b) that such small values have only a minute effect.

It is unclear at this stage what other effects (for example, corner vortices) may be present which may perhaps explain the discrepancies. Also, while great care was taken to ensure nominally zero pressure gradient conditions, the likelihood of possible local adverse pressure effects can not be totally ruled out. Further detailed local measurements of pressure gradients would be required in future work, particularly for the $AR = 1/4$ case.

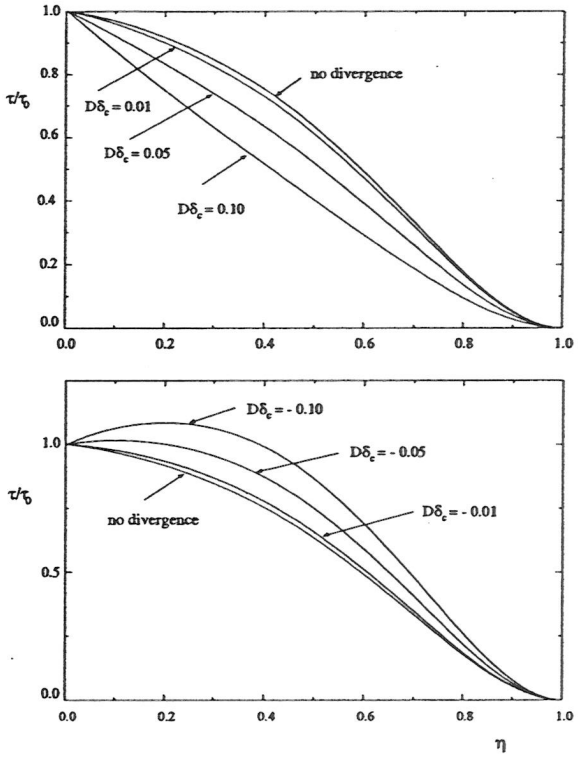

Figure 4: Shear stress profiles using equation (10) (a) Divergent flow, (b) Convergent flow.

It could well be that the close proximity of side walls with their zero normal velocity and no slip boundary conditions may be affecting the turbulence structure in some way. If such an influence is present great care needs to taken in future work to clearly isolate it.

Overall however, this preliminary investigation of aspect ratio effects suggests that turbulence structure appears to remain relatively unchanged for AR values at least below 1/7.

REFERENCES

Coles, D.E. (1956) *J. Fluid Mech.* **1**, 191–226.

Head, M.R. & Prahlad, T.S. (1974) *Aero. Q.* **25**, 293.

Perry, A.E. (1982) *Hot-wire Anemometry* Oxford Uni. Press.

Perry, A.E. & Li, J.D. (1990) *J. Fluid Mech.* **218**, 405-438.

Perry, A.E., Marusic, I., & Li, J.D. (1994). *Phys. Fluids* **2 (6)**, 1024–1035.

Saddoughi, S.G. (1988) Ph.D. Thesis, Uni. of Melbourne

Stratford, B.S. (1959) *J. Fluid Mech.* **5**, 1-16.